Mon. Not. R. Astron. Soc. **262**, 179–186 (1993)

Iron Kα lines from X-ray photoionized accretion discs

G. Matt,[1] A. C. Fabian[1] and R. R. Ross[1,2]
[1] *Institute of Astronomy, University of Cambridge, Madingley Road, Cambridge CB3 0HA*
[2] *Physics Department, College of the Holy Cross, Worcester, MA 01610, USA*

Accepted 1992 October 22. Received 1992 October 20; in original form 1992 September 9

ABSTRACT

The properties of the iron Kα line emitted by an accretion disc illuminated by an external X-ray source are calculated for different values of the disc accretion rate $\dot{m}$, and for two different source geometries: a point source located on the disc axis and an extended source above the innermost part of the disc. We find that for large values of $\dot{m}$ the matter can be significantly ionized, and the iron line equivalent width can reach values as high as 250 eV for the point source, and up to about 400 eV for the extended source; the line centroid energy, in the emitting rest frame, is significantly higher than 6.4 keV, the value for neutral iron. A further increase of $\dot{m}$ leads to a strong decrease of the line intensity, because the iron becomes fully stripped in the inner region of the disc. The line profiles in the Schwarzschild metric are also calculated, and for the point source they appear much more complex than those obtained assuming neutral matter.

Key words: accretion, accretion discs – line: profiles – galaxies: active – X-rays: galaxies – X-rays: stars.

1 INTRODUCTION

Ginga observations of Seyfert galaxies have revealed that their X-ray spectra above ~ 1 keV are more complex than was previously believed. In particular, an iron fluorescent line and a flattening of the spectrum above ~ 10 keV (the so-called high-energy bump) were observed in several sources (Pounds et al. 1990; Matsuoka et al. 1990; Piro, Yamauchi & Matsuoka 1990), and later established as common for such a class (Nandra 1991; Williams et al. 1992). Similar spectra also fit the data for some Galactic X-ray binaries well, particularly the black hole candidates (Tanaka 1991; Ebisawa et al. 1992; Done et al. 1992). These two features are generally interpreted as signatures of the reprocessing of the primary X-rays by cold matter (as predicted by Guilbert & Rees 1988 and Lightman & White 1988 and studied in detail by George & Fabian 1991 and Matt, Perola & Piro 1991), possibly distributed in an accretion disc (e.g. Matt et al. 1992).

Some sources, however, do not fit this model. Among these, the Seyfert galaxies MCG–5–23–16 (Piro, Matsuoka & Yamauchi 1992), NGC 6814 (Turner et al. 1992; Yamauchi et al. 1992) and Mrk 841 (Day et al. 1990; George et al. 1993) have iron lines with equivalent width W_α of the order of 300–400 eV, significantly larger than the value of $\lesssim 150$ eV expected from a disc subtending $\sim 2\pi$ sr (George & Fabian 1991; Matt et al. 1991) and observed in the majority of sources (e.g. Nandra 1991). Saucer-like configurations of the disc surface are not able to explain such high values (Matt et al. 1991). Explanations which invoke solid angles greater than 2π sr, anisotropic emission, partial obscuration of the primary source, or a delayed response of the reprocessing matter to variations in the primary flux, are all ruled out, at least for MCG–5–23–16 and NGC 6814, by the lack of an equally enhanced high-energy bump. Contributions from the outermost gas, likely to be present in some sources (e.g. Nandra et al. 1991), cannot explain the very short time delay (less than about 250 s) of the iron emission with respect to the primary flux in NGC 6814 (Kunieda et al. 1990). An overabundance of iron could in principle explain the enhanced ratio between line intensity and both the primary and reflected continua (Basko 1978; George & Fabian 1991; Matt et al. 1991), but the required values are implausibly high.

It was therefore suggested (Piro et al. 1992; Turner et al. 1992) that in these sources the reprocessing could arise from photoionized matter, in which case W_α is expected to be greater since the fluorescent yield of iron is greater for highly ionized species and the photoabsorption opacity at the line energy is reduced by the ionization of the lighter element. Compton reflection could in this case be relevant also at low energies, reducing the spectral contrast between direct and reprocessed continua.

In this paper, in order to compute the detailed properties of the iron Kα line, we extend the calculation of photoionized slabs made by Ross & Fabian (1993, hereafter RF) to cover a complete accretion disc and to include inclination effects. RF made use of the diffusion approximation which breaks down at low values of the ionization parameter (when recombination fronts occur in the outermost Thomson depth and photoelectric opacity becomes dominant over the Compton opacity at X-ray energies), and which is also limited in the information available on the angular distribution of the emerging flux. In the range of validity of the diffusion approximation, we have used the code described by RF to calculate the vertical ionization structure of the matter; otherwise, it was calculated by simply balancing the photoabsorption and recombination rates. The equations of Basko (1978) have then been used to obtain the line flux as a function of the inclination angle.

In Section 2 the details of the computation are presented, as well as further results for an illuminated slab. In Section 3 the calculations are applied to an accretion disc, for two different source geometries: a point source above the disc on the symmetry axis, and an extended, optically thin source above the inner part of the disc. Finally, in Section 4 the results are discussed and compared with the observations.

2 THE IRON LINE FROM AN X-RAY ILLUMINATED SLAB

To calculate the vertical ionization structure of the matter, we have used the numerical code described by RF. The geometry is a plane-parallel slab with constant density, illuminated on the top by a power-law spectrum with a cut-off at 100 keV and flux F_h, incident with an angle $\theta_0 = \cos^{-1}\mu_0$ with respect to the normal of the layer. The slab has a total Thomson depth of between 3 and 8, the exact value depending on the value of the ionization parameter, and it is illuminated on the bottom by a low-temperature Wien spectrum, which represents the quasi-thermal emission from within the accretion disc. We are interested here in the total spectrum emitted by the top layer of the slab (i.e. the 'reflection' spectrum). The main quantity which determines the ionization structure is the ionization parameter ξ, defined as

$$\xi = 4\pi F_h/n_H, \tag{1}$$

where n_H is the hydrogen number density. It must be noted that the ionization parameter so defined plays the main role in determining the ionization structure, but some differences, especially for the lighter elements, can arise from changes in the soft flux.

Since the emergent iron line is produced in the first few Thomson optical depths τ_T, we have averaged the ion abundances over $\tau_T = 3$, weighting each layer with an exponential law $\exp(-\tau_T/\mu_0)$ to take into account the decreasing importance of the matter along τ_T in reprocessing the X-rays. The code calculates the abundances of C v–vii, O v–ix, Mg ix–xiii, Si xi–xv and Fe xvi–xxvii, i.e. the most important elements and ions. However, for a detailed calculation of the iron line properties, the elements Ne, S, Ar, Ca and Ni are not completely negligible; neither are the precise fractions of the lower ionized stages of the calculated elements. This further information, and the entire ionization structure for values of ξ less than about 50, when the diffusion approximation breaks down, has been obtained by simply balancing the photoionization and the recombination rates:

$$N_{X^i}\int F_\nu \frac{\sigma_\nu(X^i)}{h\nu}\,d\nu = \alpha(X^{i+1})N_{X^{i+1}}n_H, \tag{2}$$

where the recombination coefficients α are taken from Shull & Van Steenberg (1982), and the photoabsorption cross-sections σ_ν are taken from Reilman & Manson (1979), Henke et al. (1982) and Band et al. (1990). The elemental abundances of Morrison & McCammon (1983) have been used.

Once the averaged ion fractions are calculated, the relevant photoabsorption cross-section and iron fluorescent yield have been inserted in the formulae of Basko (1978) to obtain the line intensity as a function of μ, the cosine of the polar angle of the emergent radiation. The effects of resonant trapping have been taken into account, simply assuming that all the Kα fluorescent photons emitted after the photoionization of Fe xvii–xxiii are completely destroyed (see RF). In practice, we have put the fluorescent yield for such ions equal to zero.

As well as the intensity, we have calculated the mean line energy; all the energy shifts due to Comptonization of the line photons have been neglected, as well as the broadening due to the line blending. Therefore the line emission at a given point has been assumed to be monochromatic in the rest frame of the matter.

We note that the present approach, with respect to those described in RF, treats in more detail the geometrical factors but at the expense of a poorer treatment of the physical interactions; it is probably more accurate at low values of the ionization parameter, but is partially inadequate at very high values of ξ. Nevertheless, the two approaches are grossly consistent with each other over the entire range of ξ (see below), supporting the reliability of our results. A treatment which combines the best aspects of the two methods is highly desirable, and will be the subject of future work.

In Fig. 1 we show $I_\alpha(\xi)/I_\alpha(0)$, i.e. the ratio between the line intensity at ξ and the 'cold' value, as a function of ξ, for two different values of μ_0 and for $\mu = 1$. We have assumed $n_H = 1.2 \times 10^{15}$ cm^{-3}, and a Wien law with temperature 25 eV and flux 10^{16} erg cm^{-2} s^{-1} for the soft input radiation (these values are representative of the inner part of the accretion disc in an AGN). The only free parameter is therefore the hard flux. The photon spectral index of the hard power law was taken as 1.7. The line centroid energy $E_{c\alpha}$ is also shown. As also noted by RF, the line intensity does not differ very much from the cold value for ionization parameters less than a few hundred. For these values, the iron is only slightly ionized (less than Fe xvi, the ionization state at which the main changes in the line properties occur), and the light elements are effective in absorbing the emitted fluorescence line photons. A dramatic change in the line intensities and energies occurs for ξ greater than a few hundred: first the line intensity decreases, due to the resonant trapping opacity, and then increases strongly, when the iron becomes more ionized than Fe xxiii. Meanwhile, the line energy shifts monotonically towards higher values. The increase in the intensity for $\xi \gtrsim 1000$ with respect to the cold case is due to two factors.

(i) The fluorescent yield is greater for highly ionized iron.
(ii) While the iron is highly but not completely ionized, being still effective in producing line photons, the lighter

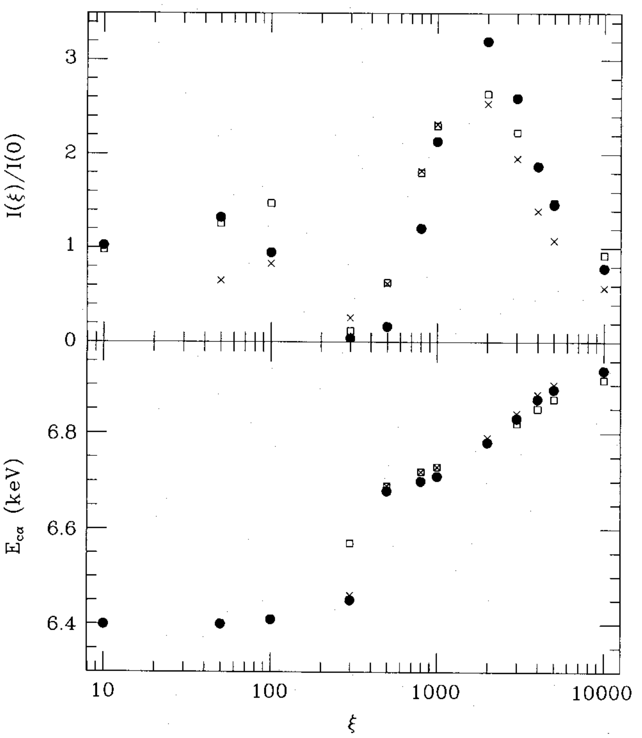

Figure 1. The intensity (normalized to the $\xi=0$ value) and the centroid energy $E_{c\alpha}$ of the iron line emitted by an X-ray illuminated slab, as a function of the ionization parameter ξ, for $\mu=1$. The crosses and the circles refer to $\mu_0=1/\sqrt{3}$ and 1 respectively, and are obtained keeping F_s at a fixed value. The squares are obtained instead if it is assumed that $F_s=F_h\,(\mu_0=1/\sqrt{3})$.

elements are almost completely bare, and therefore cannot absorb the emitted photons. Moreover, for neutral matter the iron contributes only half of the photoabsorption cross-section at its *K*-edge energy; if the lighter elements are stripped, instead, absorption by iron becomes the dominant interaction at this energy between the X-rays and the matter.

If the ionization parameter is greater than a few thousand, the iron becomes largely stripped, and iron photoabsorption becomes less important than the scattering; as a consequence, the iron line intensity decreases.

The ionization parameter, as defined in equation (1), dominates the ionization structure of the matter and therefore the line intensity. However, a less important but not always negligible role is played by the soft flux, which can contribute to the ionization of the light elements. This is shown by the open squares in Fig. 1, which are obtained by assuming $F_s=F_h(\mu_0=1/\sqrt{3})$ rather than keeping F_s fixed at a constant value. The enhancement in the ionization of the light elements produces a stronger line intensity.

Comparing our Fig. 1 with fig. 3 of RF, it can be noted that the results obtained with the two approaches are in good agreement. The value we obtain at $\xi=2000$ (which, for matter subtending 2π sr, corresponds to ~500 eV) is none the less about 20 per cent smaller than the corresponding one in RF. This is probably due to the fact that the formulae of Basko (1978) include only the unscattered and once-scattered radiation; for very high values of ξ, the line intensity is therefore underestimated.

3 THE IRON LINE FROM AN X-RAY ILLUMINATED ACCRETION DISC

We have applied the results described in the previous section to an X-ray illuminated accretion disc. The disc is assumed to be flat, with inner and outer radii r_i and r_o, and inclination angle $\theta_i=\cos^{-1}\mu_i$. All distances are expressed in units of the gravitational radius $r_g=GM/c^2$.

We have adopted a standard α-viscosity accretion disc (Shakura & Sunyaev 1973), in the version of Ross, Fabian & Mineshige (1992). If r is the radial coordinate of the disc in units of r_g, m the black hole mass in units of the solar mass, and $\dot{m}$ the accretion rate in the disc in units of the critical one (therefore $\dot{m}=L/L_{\rm Edd}$, with $L_{\rm Edd}$ the Eddington luminosity), the hydrogen density n_H (which in the adopted model is constant along the vertical coordinate), and the flux F_s emerging from the disc surface without any external illumination, can be written as (the notation is slightly different from that in Ross et al. 1992 and RF)

$$n_H=7.32\times10^{18}\,\frac{r^{3/2}\eta^2}{\dot{m}^2 m\alpha f^2(r)}\ \mathrm{cm}^{-3}, \qquad (3)$$

$$F_s=8.16\times10^{26}\,\frac{\dot{m}f(r)}{r^3\eta m}\ \mathrm{erg\,cm^{-2}\,s^{-1}}, \qquad (4)$$

where η is the conversion efficiency and $f(r)=1-\sqrt{6/r}$. We are here interested only in the surface layer of the disc, since the iron fluorescent line is produced within $\tau_T\sim$ a few. The total optical depth of the disc is much greater (a few hundred), so the surface layer does not significantly contribute to F_s. We therefore assume that the region which produces the iron line photons is illuminated on the top by the external hard radiation field, and on the bottom by a thermal soft flux F_s. The X-ray luminosity L_h is assumed equal to $\eta_h\dot{m}L_{\rm Edd}$, where η_h is introduced to take into account the (unknown) fraction between hard and soft luminosities.

We have studied two different source geometries. The first consists of a point source, located at a distance h above the disc on its symmetry axis; this is the geometry adopted in previous works on the iron line properties from neutral matter (George & Fabian 1991; Matt et al. 1991). The second geometry we have studied consists of an extended, optically thin source above the innermost part of the disc. The source is assumed to be a geometrically thin layer ($H\ll r$, where H is the height of the layer), located very close to the disc surface: therefore only the regions of the disc below the source are illuminated by the hard photons. Such a geometry could be representative of two-phase models, in which hot electrons in a thin corona Comptonize the soft photons coming from the underlying accretion disc (e.g. Haardt & Maraschi 1991). Obviously, these two choices do not exhaust all the possible source geometries, but they are representative of situations in which the whole disc or only its inner region is effective in reprocessing the X-rays.

In both cases the source is assumed to emit isotropically a power-law spectrum up to 100 keV with a photon spectral index equal to 1.7.

3.1 Point source

In this geometry, the ionization parameter ξ, defined in equation (1), has the following dependence on r:

$$\xi(r) = 8.97 \times 10^8 \left(\frac{\dot{m}^3 \eta_h \alpha}{\eta^2} \right) f^2(r) r^{-3/2} g(r, h), \quad (5)$$

where $g(r, h)$ describes the illumination of the disc by the central source. If the effects of light bending are neglected, $g(r, h) = h/(r^2 + h^2)^{3/2}$, and therefore $\xi(r)$, for large radii, is proportional to $r^{-9/2}$. At very small radii, ξ cannot be very high because of the factor $f(r)$. The maximum occurs around $r = 10$.

The ionization parameter depends on the factor $\dot{m}^3 \eta_h \alpha / \eta^2$. In the following, we assume $\alpha = 0.1$, $\eta = 0.06$ (valid for a Schwarzschild black hole; note that for a Kerr black hole the ionization parameter is smaller) and $\eta_h = 1$, and study the iron line properties as a function of $\dot{m}$. We present results up to $\dot{m} = 1$, to point out the effects of very high values of the ionization parameter, but one must recall that the thin-disc approximation breaks down for $\dot{m} \gtrsim 0.5$.

In Fig. 2 we show the equivalent width W_α (with respect to the direct continuum) and the centroid energy $E_{c\alpha}$ of the iron line as a function of $\dot{m}$, for three values of the black hole mass (10, 10^6 and 10^9 $M_\odot$) and without any relativistic or kinematic corrections. The plotted values refer to a face-on disc, and are obtained for $r_i = 6$, $r_o = 1000$ and $h = 20$.

From the inspection of the figure, some general points can be made.

(i) For $\dot{m}$ less than about 0.1, the matter has low ionization everywhere, and W_α is close to ~ 150 eV, the value for the neutral case (George & Fabian 1991; Matt et al. 1991). For increasing $\dot{m}$, the inner region becomes mainly populated by Fe XVII–XXIII and W_α decreases due to the resonant trapping. When $\dot{m}$ increases further, the inner part of the disc becomes highly ionized, and W_α first increases up to a maximum (at $\dot{m} \sim 0.2$–0.4, the exact value depending on m), and then decreases. This behaviour can be easily understood on the basis of the results discussed in the previous section.

(ii) W_α can reach values as high as ~ 250 eV, much higher than the cold value for the same set of parameters (Matt et al. 1992). The low ionization of the matter in the outer part of the disc prevents higher values of W_α.

(iii) The ionization parameter does not depend on the black hole mass, but the soft flux increases with decreasing m (equation 4). Thus, for a decrease of m, the ionization of the matter (and in particular of the light elements) increases, and for a stellar-mass black hole the maximum of W_α is reached at a smaller value of $\dot{m}$.

(iv) The centroid energy of the line increases with $\dot{m}$, varying sharply from about 6.4 keV (the cold value) to 6.6–6.7 keV.

The equivalent width and the centroid energy as a function of μ_i, the cosine of the inclination angle, are shown

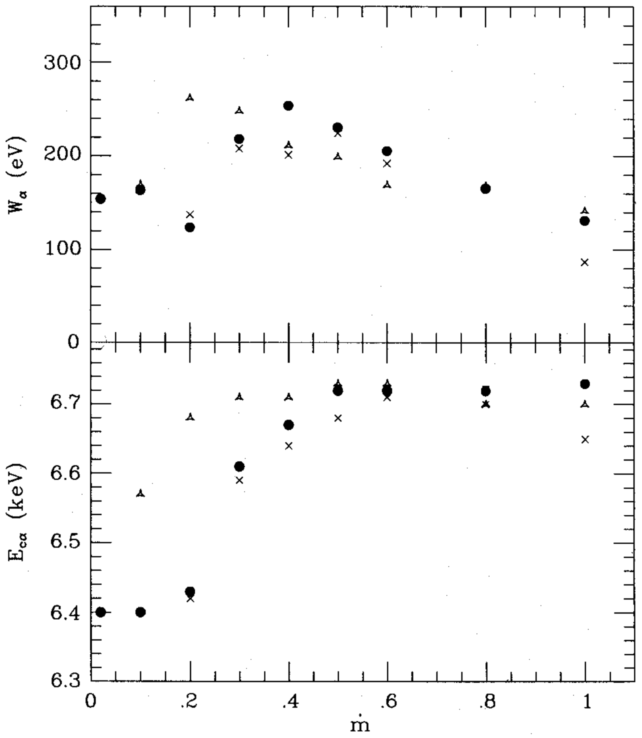

Figure 2. The equivalent width W_α and the centroid energy $E_{c\alpha}$, without the relativistic correction, for a face-on disc, as a function of $\dot{m} = L/L_{Edd}$. The adopted source geometry is a point located at height $h = 20$ on the disc axis. The triangles refer to a black hole with $m = 10$, the circles to $m = 10^6$ and the crosses to $m = 10^9$. The inner and outer radii of the disc are 6 and 1000.

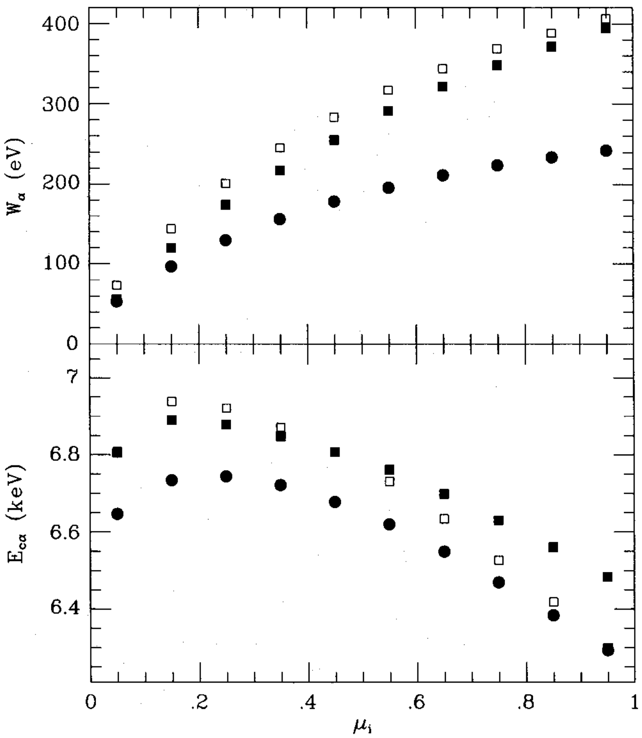

Figure 3. W_α and $E_{c\alpha}$ as a function of the cosine of the inclination angle, μ_i, for a black hole mass of 10^6 when the relativistic effects are taken into account. The filled circles are obtained in the point-source geometry for $\dot{m} = 0.4$, while the squares are obtained with the extended-source geometry: $r_2 = 30$, $\dot{m} = 0.25$ (open) and $r_2 = 50$, $\dot{m} = 0.4$ (filled).

in Fig. 3 (filled circles), for $m = 10^6$ and $\dot{m} = 0.4$, when the kinematic and relativistic effects (in the Schwarzschild metric: see Fabian et al. 1989 and Chen & Eardley 1991) are taken into account. It should be noted that transverse Doppler and gravitational redshifts shift the centroid energy for small inclination angles to values of the order of 6.4 keV or less. At very high inclination angles, the centroid energy turns down due to the enhanced contribution of the photons emitted at the far side of the disc (Matt et al. 1992; Matt, Perola & Stella 1993).

The dependence on the radial coordinate of the ionization parameter results in a dramatic change of the radial law of the line emissivity with respect to the cold case. The weight of the inner part of the disc can be strongly enhanced, and the line energy (in the rest frame) varies with r. These factors have a strong impact on the line profile. In Fig. 4 we show the line profiles for two values of the inclination angle (30° and 70°) and three values of $\dot{m}$ ($\ll 1$, 0.4 and 0.8) for a black hole with $m = 10^6$. The profiles for ionized discs are much more complex than in the cold case. In fact, if $\dot{m}$ is sufficiently high, the disc can roughly be divided into three parts: an inner region, with a strong line emission and a line energy (in the rest frame) of 6.6–6.9 keV; an intermediate region with a very low intensity (due to resonant trapping) and a centroid energy greater than the neutral value; and an outer part with a line intensity and energy close to the cold values. Since the transition between the region in which $E_{c\alpha}$ is greater than 6.6 keV and that in which $E_{c\alpha} \sim 6.4$ keV is sharp, the resulting

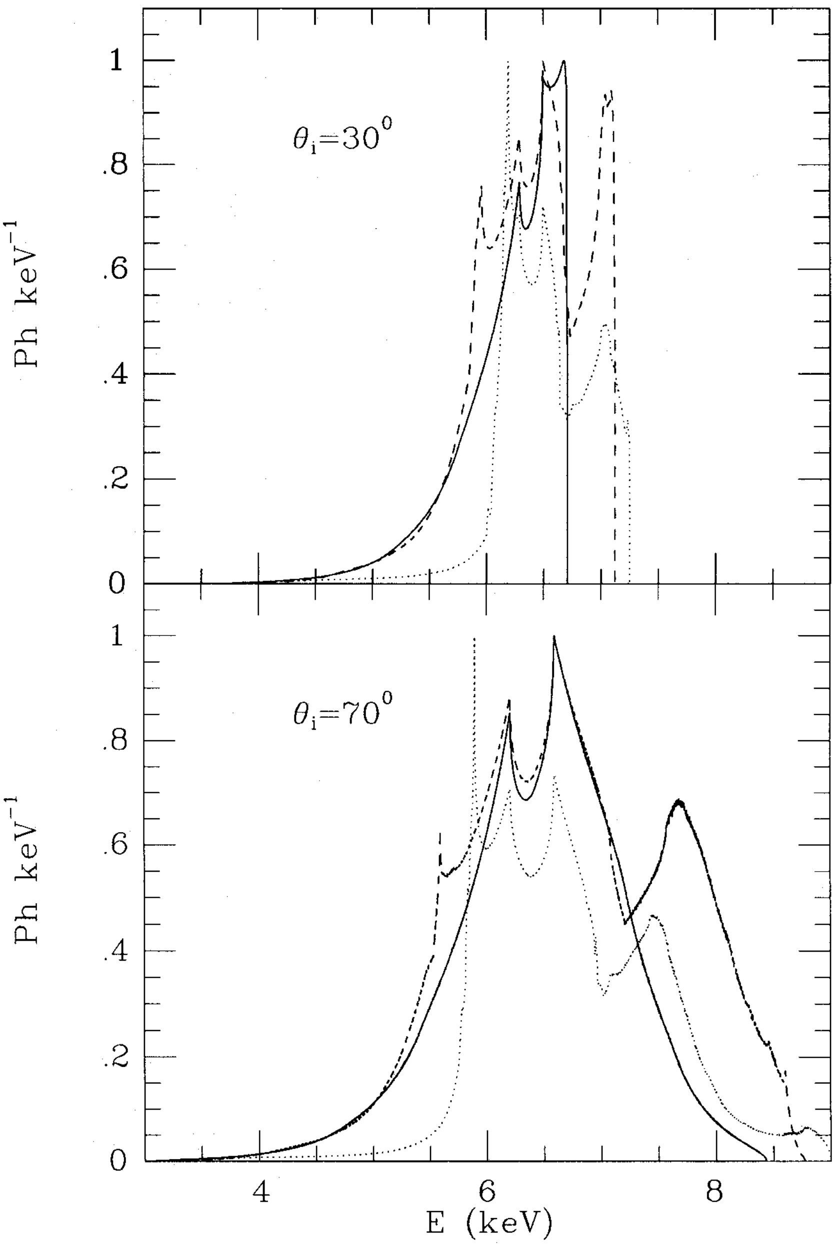

Figure 4. The line profiles for $\dot{m} = 0.4$ (dashed curves) and $\dot{m} = 0.8$ (dotted curves), and for two values of the inclination angle θ_i, for the point-source geometry. $h = 20$, $m = 10^6$, $r_i = 6$, $r_o = 1000$. The cold case ($\dot{m} \ll 1$, solid curves) is also shown for comparison.

profile is practically the sum of two different contributions, each of these with basically a double-peaked structure. Another important difference with respect to the cold case is the fact that, for very highly ionized discs, the red peaks can be brighter than the blue ones.

3.2 Extended source

We assumed that the source extends from r_1 to r_2, and that each point in the emitting ring has the same luminosity. Contrary to the point-source geometry, each point on the disc is now illuminated by the same, isotropic radiation field. For simplicity, we have represented the isotropic illumination by assuming $\mu_0 = 1/\sqrt{3}$. The radial dependence of the ionization parameter is now dictated only by the density, and is given by

$$\xi(r) = \begin{cases} 1.79 \times 10^9 (\dot{m}^3 \eta_h \alpha / \eta^2) f^2(r) r^{-3/2} (r_2^2 - r_1^2)^{-1} & r \le r_2; \\ 0 & r > r_2. \end{cases} \quad (6)$$

In the following we assume $r_1 = r_i = 6$. In this geometry the ionization parameter spans a much narrower range of values along r than in the point-source geometry. This results in a greater range of the equivalent-width values when $\dot{m}$ varies, because there is no contribution from the cold outermost regions. W_α and $E_{c\alpha}$ are shown in Fig. 5 for $r_2 = 30$ (open squares) and $r_2 = 50$ (filled squares). Now W_α can be very low (for instance, about 40 eV for $r_2 = 50$ and $\dot{m} = 0.2$), but can reach values as high as 400 eV (for $r_2 = 50$ and $\dot{m} = 0.4$ or $r_2 = 30$ and $\dot{m} = 0.25$). Since ξ increases as r_2 decreases, for $r_2 = 30$ the maximum in W_α occurs at a lower value of $\dot{m}$ than for $r_2 = 50$. The values of $E_{c\alpha}$ are greater than those obtained in the point-source geometry.

The equivalent width and the centroid energy as a function of μ_i are shown in Fig. 3 for those values of $\dot{m}$ for which the maxima in W_α occur, assuming $m = 10^6$, and including the kinematic and relativistic corrections. If $r_2 = 50$, W_α is greater than 300 eV for $\mu_i \gtrsim 0.5$, while the centroid energy is always greater than 6.4 keV; for $r_2 = 30$, W_α is smaller and $E_{c\alpha}$, due to the stronger effects of the gravitational and Doppler transverse redshifts and of Doppler boosting, spans a wider range of values.

Because ξ does not vary very much with r, the centroid energy is almost constant along the radial coordinate. Therefore the line profiles exhibit the usual double-peaked structure, as can be seen in Fig. 6; the only significant difference with respect to the cold case is a shift towards higher energies. The profiles therefore represent a powerful diagnostic with which to study the geometry of the X-ray source.

4 DISCUSSION AND CONCLUSIONS

The iron Kα is the most important line in the X-ray band, and it provides information on the physics and geometry of the very central region of AGN and X-ray binaries. Its properties in the X-ray illuminated accretion disc picture have been studied in detail by George & Fabian (1991), Matt et al. (1991) and Matt et al. (1992) in the $\xi = 0$ limit.

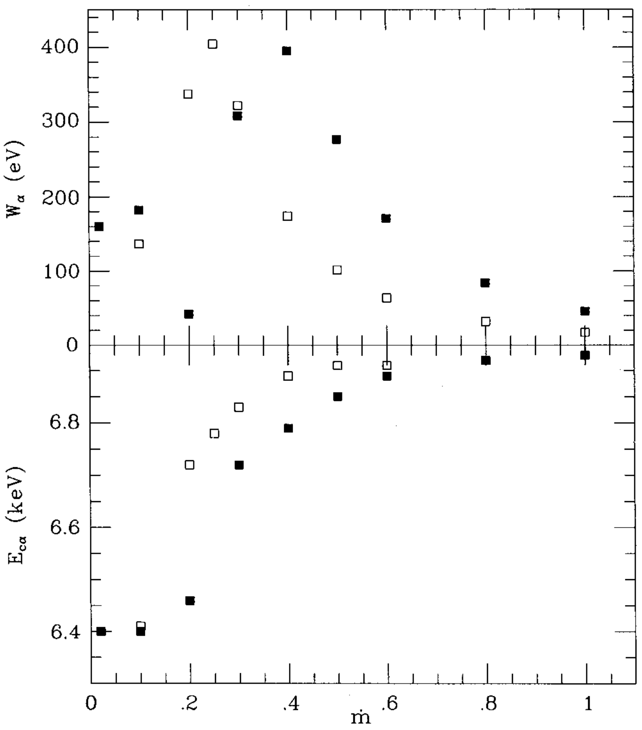

Figure 5. The equivalent width W_α and the centroid energy $E_{c\alpha}$, without the relativistic correction, for a face-on disc, as a function of $\dot{m}$ for the extended-source geometry. $m = 10^6$, $r_1 = r_i = 6$, $r_2 = 30$ (open squares) or 50 (filled squares).

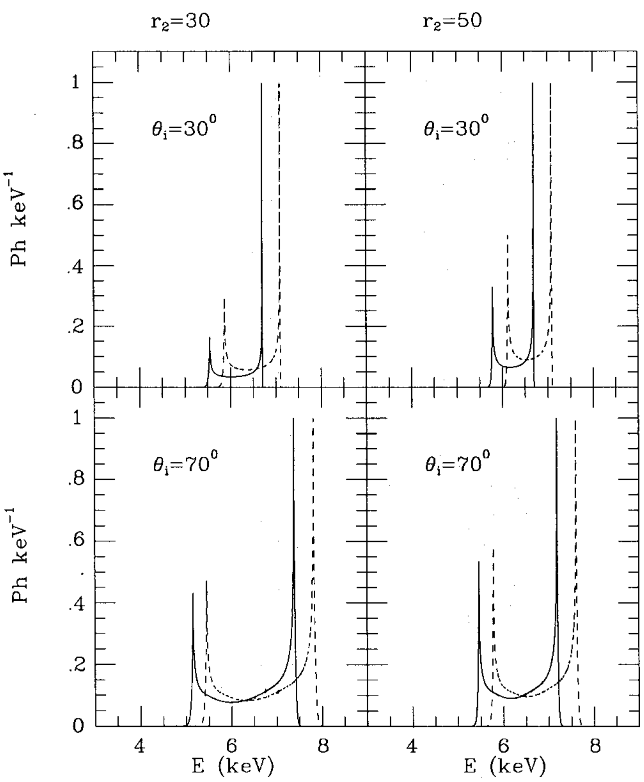

Figure 6. The line profiles for $\dot{m} \ll 1$ (solid curves) and for $\dot{m} = 0.25$ (0.4)(dashed curves) for an extended source with $r_2 = 30$ (50), for two values of θ_i. $m = 10^6$, $r_1 = r_i = 6$.

In this paper, we have calculated the iron Kα line properties from an accretion disc illuminated by a hard flux strong enough to ionize the matter significantly. The present results are based on a simple approach; the main approximations are given below.

(i) We have calculated in detail the vertical ionization structure of the matter, but have then used an averaged value to compute the line intensity.

(ii) Following Basko (1978), we have included in the calculations of the line intensity only the unscattered and once-scattered line photons. This is certainly a very good approximation for low values of ξ, but could lead to an underestimation of the line intensity at higher ξ.

(iii) Line broadening due to the Comptonization of line photons has been neglected, as well as that due to line blending. The true line profiles are therefore probably broader and smoother than those shown in Figs 4 and 6.

(iv) We have calculated the equivalent width with respect to the direct continuum, because a detailed calculation of the reflected continuum is beyond the scope of this paper. This fact must be borne in mind when comparing the values presented here with the observed ones.

The present results are certainly adequate to understand the main properties and dependences of the iron line from an ionized disc. A more detailed computation is not required by the quality of the present data, which are obtained with detectors with modest energy-resolution. In fact, it must be noted that the uncertainties on the measured line intensities are not merely statistical, but arise also from the difficulties of distinguishing between the line and continuum contributions: see, for instance, the dramatic variations of the equivalent width in NGC 6814 for changes of the fitted model (Turner et al. 1992). On the other hand, looking forward to the high energy-resolution, high-sensitivity missions scheduled for the near future, a detailed computation which joins a careful treatment of the geometry and the physics would be highly desirable. This will require a different and more expensive (in terms of human and computer time) approach, which we intend to attempt later.

The observed values of W_α ($\sim 350 \pm 50$ eV) and $E_{c\alpha}$ ($\sim 6.4 \pm 0.1$ keV) for both NCG-5-23-16 (Piro et al. 1992) and NGC 6814 (Turner et al. 1992; but see the uncertainties mentioned above) are only marginally in agreement with those shown in Fig. 3 for small inclination angles, if the point-source model is adopted. In fact, from our calculations we obtain values of W_α somewhat smaller than those observed (which are in general calculated with respect to the total continuum), but, as discussed, our present approach probably underestimates the line intensity, in particular at high values of ξ. In any case, a good agreement can be obtained simply by making small changes in the geometry (i.e. more irradiation of the inner part of the disc), or by assuming an iron abundance which is not dramatically greater than the solar one. If we adopt the extended source geometry, values of W_α in agreement with those observed are obtained for a wide range of μ_i, but the centroid energies are somewhat higher than those observed, at least for $r_2 = 50$. Measurements of detailed line profiles seem necessary in order to distinguish between the two source-models (see Figs 4 and 6). The lack of a high-energy excess in these two sources can also be interpreted in terms of reflection and thermal emission from an X-ray illuminated, ionized disc (see RF), in that the reduced spectral contrast between direct and reflected radiations makes the reflected component difficult to observe. It must also be noted that the reprocessing of the primary X-rays from ionized matter seems to be able to explain (RF) the spectra of some Galactic black hole candidates, and in particular Cygnus X-1 (Tanaka 1991; Ebisawa et al. 1992).

The upper limit of about 250 s on the time delay between line and continuum variations in NGC 6814 (Kunieda et al. 1990) is also consistent with the ionized disc interpretation. While for a cold, centrally illuminated disc about half of the line photons are emitted within about $50 r_g$ (Matt et al. 1991), for an ionized disc the contribution of the innermost part of the disc is much larger. Obviously, the extended-source geometry leads naturally to almost simultaneous continuum and line emission.

Only for relatively high values of $\dot{m}$ do we find line properties which differ significantly from the neutral case: this is consistent with the fact that anomalously strong lines have been observed in only a few objects, at least among Seyfert 1 galaxies. In high-luminosity quasars, which do not show, as a class, clear evidence of reprocessing (Williams et al. 1992), the value of $\dot{m}$ could be close to 1 (or η_h much greater than 1), although alternative explanations (i.e. beaming) are possible.

ACKNOWLEDGMENTS

We thank G. C. Perola and L. Piro for several discussions, and A. Fazzolari for kindly providing some software facilities. ACF and GM acknowledge financial support by the Royal Society and by a NATO/CNR fellowship respectively.

REFERENCES

Band I. M., Trzhaskovskaya M. B., Verner D. A., Yakovlev D. G., 1990, A&A, 237, 267
Basko M. M., 1978, ApJ, 223, 268
Chen K., Eardley D. M., 1991, ApJ, 382, 125
Day C. S. R., Fabian A. C., George I. M., Kunieda H., 1990, MNRAS, 247, 15P
Done C., Mulchaey J. S., Mushotzky R. F., Arnaud K. A., 1992, ApJ, 395, 275
Ebisawa K., Inoue H., Mitsuda K., Nagase F., Tanaka Y., Yaqoob T., Yoshida K., 1992, in Tanaka Y., Koyama K., eds, Frontiers of X-ray Astronomy. Universal Academy Press, Tokyo, p. 301
Fabian A. C., Rees M. J., Stella L., White N. E., 1989, MNRAS, 238, 729
George I. M., Fabian A. C., 1991, MNRAS, 249, 352
George I. M., Nandra K., Fabian A. C., Turner T. J., Done C., Day C. S. R., 1993, MNRAS, 260, 111
Guilbert P. W., Rees M. J., 1988, MNRAS, 233, 475
Haardt F., Maraschi L., 1991, ApJ, 380, L51
Henke B. L., Lee P., Tanaka T. J., Shimabukuro R. L., Fujikawa B. K., 1982, At. Data Nucl. Data Tables, 27, 1
Kunieda H., Turner T. J., Awaki H., Koyama K., Mushotzky R. F., Tsusaka Y., 1990, Nat, 345, 786
Lightman A. P., White T. R., 1988, ApJ, 335, 57
Matsuoka M., Piro L., Yamauchi M., Murakami T., 1990, ApJ, 361, 440
Matt G., Perola G. C., Piro L., 1991, A&A, 247, 25
Matt G., Perola G. C., Piro L., Stella L., 1992, A&A, 257, 63 (Erratum in A&A, 263, 453)

Matt G., Perola G. C., Stella L., 1993, A&A, 267, 643
Morrison R., McCammon D., 1983, ApJ, 270, 119
Nandra K., 1991, PhD thesis, Univ. Leicester
Nandra K., Pounds K. A., Stewart G. C., George I. M., Hayashida K., Makino F., Ohashi T., 1991, MNRAS, 248, 760
Piro L., Yamauchi M., Matsuoka M., 1990, ApJ, 360, L35
Piro L., Matsuoka M., Yamauchi M., 1992, in Duschl W. J., Wagner S. J., eds, Physics of Active Galactic Nuclei. Springer-Verlag, Berlin, p. 45
Pounds K. A., Nandra K., Stewart G. C., George I. M., Fabian A. C., 1990, Nat, 344, 132
Reilman R. F., Manson S. T., 1979, ApJS, 40, 815
Ross R. R., Fabian A. C., 1993, MNRAS, in press (RF)
Ross R. R., Fabian A. C., Mineshige S., 1992, MNRAS, 258, 189
Shakura N. I., Sunyaev R. A., 1973, A&A, 24, 337
Shull J. M., Van Steenberg M., 1982, ApJS, 48, 95
Tanaka Y., 1991, in Treves A., Perola G. C., Stella L., eds, Iron Line Diagnostics in X-ray Sources. Springer-Verlag, Berlin, p. 98
Turner T. J., Done C., Mushotzky R., Madejski G., 1992, ApJ, 391, 102
Williams O. R. et al., 1992, ApJ, 389, 157
Yamauchi M., Matsuoka M., Kawai N., Yoshida A., 1992, ApJ, 395, 453